Mean-Field Calculations of Chain Packing and Conformational Statistics in Lipid Bilayers: Comparison with Experiments and Molecular Dynamics Studies

Deborah R. Fattal and Avinoam Ben-Shaul
Department of Physical Chemistry and the Fritz Haber Research Center, The Hebrew University of Jerusalem, Jerusalem 91904, Israel

ABSTRACT A molecular, mean-field theory of chain packing statistics in aggregates of amphiphilic molecules is applied to calculate the conformational properties of the lipid chains comprising the hydrophobic cores of dipalmitoyl-phosphatidylcholine (DPPC), dioleoyl-phosphatidylcholine (DOPC), and palmitoyl-oleoyl-phosphatidylcholine (POPC) bilayers in their fluid state. The central quantity in this theory, the probability distribution of chain conformations, is evaluated by minimizing the free energy of the bilayer assuming only that the segment density within the hydrophobic region is uniform (liquidlike). Using this distribution we calculate chain conformational properties such as bond orientational order parameters and spatial distributions of the various chain segments. The lipid chains, both the saturated palmitoyl ($-(CH_2)_{14}-CH_3$) and the unsaturated oleoyl ($-(CH_2)_7-CH=CH-(CH_2)_7-CH_3$) chains are modeled using rotational isomeric state schemes. All possible chain conformations are enumerated and their statistical weights are determined by the self-consistency equations expressing the condition of uniform density. The hydrophobic core of the DPPC bilayer is treated as composed of single (palmitoyl) chain amphiphiles, i.e., the interactions between chains originating from the same lipid headgroup are assumed to be the same as those between chains belonging to different molecules. Similarly, the DOPC system is treated as a bilayer of oleoyl chains. The POPC bilayer is modeled as an equimolar mixture of palmitoyl and oleoyl chains. Bond orientational order parameter profiles, and segment spatial distributions are calculated for the three systems above, for several values of the bilayer thickness (or, equivalently, average area/headgroup) chosen, where possible, so as to allow for comparisons with available experimental data and/or molecular dynamics simulations. In most cases the agreement between the mean-field calculations, which are relatively easy to perform, and the experimental and simulation data is very good, supporting their use as an efficient tool for analyzing a variety of systems subject to varying conditions (e.g., bilayers of different compositions or thicknesses at different temperatures).

INTRODUCTION

The molecular structure of lipid bilayers is a subject of continuous intensive experimental and theoretical research (for reviews see, e.g., Bloom et al., 1991; Lipowsky and Sackmann, 1994). The study of such topics as lipid headgroup interactions and chain conformational statistics, and their dependence on membrane composition, thickness, and curvature, is of great biological importance, e.g., for the understanding of membrane phase transitions, lipid-protein interaction, solubilization of hydrophobic solutes, or bilayer curvature elasticity. The theoretical approaches for treating these issues involve a variety of continuum theories and molecular models (see, e.g., Ben-Shaul and Gelbart, 1994). The latter range from simple (yet often very useful) molecular packing considerations (Israelachvili, 1985) to very detailed molecular dynamics (MD) simulations (see, e.g., van der Ploeg and Berendsen, 1983; Heller et al., 1993). Intermediate between these two extremes are mean-field theories in which the conformational properties of any given molecule are calculated subject to the averaged influence (the mean-field) of its neighbors (Marčelja, 1974; Dill et al., 1988; Gruen, 1985a,b; Ben-Shaul et al., 1985; Szleifer et al., 1985).

Unlike MD simulations, mean-field theories of molecular packing in lipid membranes cannot provide dynamical information on molecular motions (except indirectly; see Results and Analysis, below). Also, they treat only approximately thermodynamic properties, such as membrane phase transitions (Marčelja, 1974) or mechano-thermodynamic characteristics such as curvature and stretching elasticities (Szleifer et al., 1990; Ennis, 1992). Yet, at present, they provide the most efficient (and quite reliable) means of studying these phenomena. This is because even the most advanced MD simulations to date are limited to relatively short time scales (hundreds of picoseconds) and to few specific systems under special conditions (see, e.g., Heller et al., 1993, and references therein).

On the other hand, using mean-field theories, e.g., of the kind described in this paper, it is rather easy to analyze a large number of systems subject to various conditions (involving, for instance, molecular composition, bilayer thickness, chain length, and curvature of the membranes). Some mean-field theories provide explicit expressions for the probability distributions of molecular conformations and related properties, thus allowing for qualitative insights into the underlying physics. Also, mean-field theories can provide detailed and reliable information on various "single-chain" (conformational) properties such as bond orientational order parameter profiles of the lipid acyl chains or spatial distributions of the various chain segments (Gruen 1985a,b; Szleifer et al., 1985). Possibly, the probability distribution of molecular conformations predicted by mean-field theories may be used

Received for publication 21 March 1994 and in final form 2 June 1994.
Address reprint requests to Avinoam Ben-Shaul, Department of Physical Chemistry, The Hebrew University of Jerusalem, Fritz Haber Research Center for Molecular Dynamics, Jerusalem 91904, Israel. 972 2 585271 Fax: 972 2 513742; E-mail: abs@batata.fh.huji.ac.il.
© 1994 by the Biophysical Society
0006-3495/94/09/983/13 $2.00

as initial distributions in many-molecule calculations, to enhance the convergence of MD and Monte Carlo simulations.

In this paper we employ a mean-field theory to calculate the conformational properties of the acyl chains in the hydrophobic cores of some typical lipid bilayers, involving dipalmitoyl-phosphatidylcholine (DPPC), dioleoyl-phosphatidylcholine (DOPC), and palmitoyl-oleoyl-phosphatidylcholine (POPC) as the constituent molecules. This theory, whose basic concepts are outlined in the next section, has previously been used to calculate various conformational and thermodynamic properties of amphiphile chains in micelles, monolayers, and bilayers, including, e.g., orientational bond order parameter profiles in various aggregation geometries, chain packing statistics in mixed bilayers, curvature elastic moduli (Szleifer et al., 1990), and lipid-protein interaction (Fattal and Ben-Shaul, 1993). In all these applications, however, only fully saturated hydrocarbon chains have been considered. In this paper we employ the theory to study lipid bilayers composed of both saturated and monounsaturated acyl chains. Our main objective is to test the theory by comparing its predictions to some recent (and some less recent) experimental (Kõnig et al., 1992; Wiener and White, 1992a,b; Seelig and Waespe-Šarčević, 1978) and theoretical studies (Heller et al., 1993), and demonstrate its potential for calculating lipid conformational properties for systems of biological relevance.

THEORY

The calculations presented in this paper in Results and Analysis are concerned with the conformational properties of the lipid acyl chains within the hydrophobic core of the bilayer. More specifically, we shall be mainly concerned with the bond orientational order parameters of the hydrocarbon chains and with the spatial distribution of their various segments (methyl groups, methylene groups, and double bonds). In every calculation presented we shall consider a given cross-sectional area per lipid chain (or headgroup) a, chosen generally according to the experimental or theoretical study with which the results will be compared. We shall not consider headgroup interactions, which (together with chain-chain interactions) determine the equilibrium area per molecule a (Dill and Stigter, 1988; Stigter and Dill, 1988; Winterhalter and Helfrich, 1992; Ennis, 1992; Andelman, 1994; Fattal and Ben-Shaul, 1993; Ben-Shaul, 1994). In other words, we shall treat a as a "boundary condition" in our calculations. If, as usual, the hydrophobic core of the bilayer (in its fluid, liquid-crystalline state) is assumed to be characterized by a uniform, liquidlike density of hydrophobic segments (Tanford, 1980; Israelachvili, 1985; Wennerström and Lindman, 1979), then a is simply related to the thickness d of the bilayer; namely $a = d/2v = \ell/v$ where $\ell = d/2$ is the average length of the hydrophobic tail of the lipid and v is its volume. As will become apparent from the formalism below, the theory employed in this paper does not involve adjustable parameters nor any assumptions besides that of uniform average segment density within the hydrophobic core. (The uniform density constraint can be relaxed, e.g., when dealing with dense monolayers, where the density profile decreases toward the chain ends (Ben-Shaul and Gelbart, 1994)).

The basic quantity in our model is the probability distribution of chain conformations, $P(\alpha)$. A given chain conformation $\alpha = b, \Omega, x_0$ is characterized by 1) the bond sequence of the hydrocarbon tail, b, e.g., the *trans/gauche* sequence in the case of saturated alkyl chains (Flory, 1969); 2) the overall orientation of the chain relative to a bilayer's fixed system of coordinates, Ω, (three Euler angles, θ, ϕ, and ψ, specify Ω; two angles specifying the orientation of the end-to-end vector of the chain relative to the normal to the bilayer plane; and one measuring the rotation of the molecule around this vector); and 3) the position of the headgroup (more precisely, the origin of the chain), x_0, along the normal to the membrane's plane; see Fig. 1.

In a bilayer composed of several different hydrocarbon chains i, with corresponding possible conformations $\{\alpha_i\}$, every chain species will be characterized by its own conformational probability distribution $P(\alpha_i)$ (Szleifer et al., 1987). Similarly, the two chains constituting the hydrophobic tail of a phospholipid molecule are generally nonequivalent (Elder et al., 1977; Büldt et al., 1978; Seelig and Waespe-Šarčević, 1978; Seelig and Seelig, 1980; Hauser et al., 1981), and thus involve different probability distributions. In all the calculations presented in the next section we shall consider only "pure" (single lipid) bilayers composed of doubly chained lipid tails. If the two lipid chains are different, such as the oleoyl and palmitoyl chains of POPC, we shall treat the system as an equimolar binary mixture of the two chains characterized by two different conformational distributions $P(\alpha_1)$ and $P(\alpha_2)$. If the two lipid chains have the same chemical structure, as in the case of DPPC or DOPC, the bilayer will be regarded as composed of one type of chain (thus ignoring the fact that, e.g., the two oleoyl chains in DOPC are not entirely equivalent; see next section). Alternatively, we could define $P(\alpha)$ as the conformational distribution of the whole lipid (doubly chained) tail; yet computationally it is simpler to consider each of the two lipid chains as a different component.

The derivation of our expression for $P(\alpha_i)$ has been described in detail elsewhere (Ben-Shaul et al., 1985; Ben-

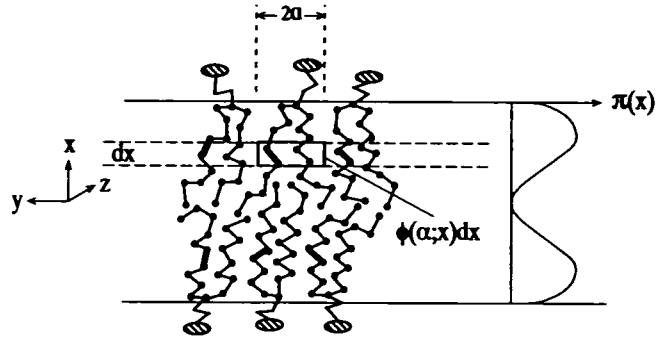

FIGURE 1 A schematic illustration of a lipid bilayer and the quantities appearing in the singlet probability distribution of chain conformations.

Shaul and Gelbart, 1994; for alternative mean-field/single-chain theories, see, e.g., Gruen, 1985a,b; and Dill et al., 1988). Thus we shall first state the result, then write the (self-consistency) equations one needs to solve to evaluate the molecular-thermodynamic parameters appearing in $P(\alpha_i)$ and, finally, discuss how the $P(\alpha_i)$ can be used to calculate the free energy and chain conformational properties of the bilayer. Going backward it will then become apparent how $P(\alpha_i)$ can be derived by minimizing the free energy of the system.

The conformational probability distribution of a chain of type i is given by

$$P(\alpha_i) = \frac{1}{q_i}\exp\left[-\beta\epsilon(\alpha_i) - \beta\int \pi(x)\varphi(x;\alpha_i)\,dx\right] \quad (1)$$

Here $\beta = 1/kT$ is the reciprocal temperature, with k denoting Boltzmann's constant, and q_i is an (isothermal-isobaric) partition function ensuring that $P(\alpha_i)$ is normalized, i.e., $\sum_{\alpha_i} P(\alpha_i) = 1$. $\epsilon(\alpha_i)$ is the internal (*trans/gauche*) energy of a chain in conformation α_i and $\varphi(x;\alpha_i)dx$ is the volume occupied by this chain within a thin shell of thickness dx parallel to the plane of the bilayer and at a distance x from the midplane of the bilayer; see Fig. 1. For alkyl chains composed of different types of segments s, ($s = CH_2$, CH_3 or CH groups), $\varphi(x;\alpha_i) = \sum_s \psi_s(x;\alpha_i)v_s$, with $\psi_s(x;\alpha_i)\,dx$ denoting the number of s segments of an α_i chain whose centers fall between x and $x + dx$, and v_s is the specific volume per segment in the liquid hydrocarbon phase. The commonly accepted values for —CH_2—, —CH_3 and —CH=CH— segments are $v \simeq 27$ Å^3, 54 Å^3, and 43 Å^3, respectively (Nagle and Wilkinson, 1978; Wilkinson and Nagle, 1981; Lewis and Engelman, 1983; Nagle and Wiener, 1988; Wiener and White, 1992a. For other values see, for example, Small, 1986). It should be noted, however, that v_s does not appear explicitly in our calculations. It is only used to relate the hydrophobic thickness d of the bilayer to the average area per molecule a; namely $d/2 = v/a$ where v is the volume of the tail. Explicitly, $v = \sum_s n_s v_s$ where n_s is the number of s segments per molecule. (Note $n_s = \int dx\,\psi_s(x;\alpha_i)$ is independent of α_i). It is the thickness of the bilayer d that enters as an explicit input parameter into the calculations. The integration limits in Eq. 1 extend over the hydrophobic region, i.e., from $-d/2$ to $+d/2$.

The function $\pi(x)$ appearing in Eq. 1 is the lateral pressure (or stress) profile acting on the chains within the hydrophobic core. It accounts for the reduced conformational freedom of the chains because of interchain excluded volume interactions or, in other words, because of the tight packing conditions within the membrane. The numerical values of the $\pi(x)$ are determined by the self-consistency equations (the "packing constraints"), representing the requirement for uniform hydrocarbon density within the hydrophobic core. More explicitly, consider a portion of a planar bilayer of total area A, and let N_i^u and N_i^ℓ denote the number of chains of type i originating from the "upper" ($x = +d/2$) and "lower" ($x = -d/2$) interfaces of the bilayer, respectively. Consider now a thin layer x, $x + dx$ of volume $A(x)\,dx = A\,dx$, parallel to the plane of the bilayer. The contribution of i chains originating at the upper interface to the segment density in this volume is $N_i^u\langle\varphi_i^u(x)\rangle\,dx$, with $\langle\varphi_i^u(x)\rangle = \sum_{\alpha_i} P^u(\alpha_i)\varphi^u(x;\alpha_i)$. The corresponding contribution from chains originating at the lower interface is $N_i^\ell\langle\varphi_i^\ell(x)\rangle\,dx = N_i^\ell\sum_{\bar\alpha_i} P^\ell(\bar\alpha_i)\varphi^\ell(x;\bar\alpha_i)dx$ with $\bar\alpha_i$ denoting the conformations of i-chains originating from the ℓ-interface. Note that there is a one-to-one correspondence between the α_i and the $\bar\alpha_i$ via reflection through the midplane. Using $\bar\alpha_i$ to denote the mirror image of α_i we have $\varphi^u(x;\alpha_i) = \varphi^\ell(-x;\bar\alpha_i)$ and hence also $\varphi^\ell(x;\bar\alpha_i) = \varphi^u(-x;\alpha_i)$. Note further that for a symmetric bilayer, (corresponding to $N_i^u = N_i^\ell = N_i$ for all i) we have $P^u(\alpha_i) = P^\ell(\bar\alpha_i) \equiv P(\alpha_i)$ and $\langle\varphi_i^u(x)\rangle = \langle\varphi_i^\ell(-x)\rangle \equiv \langle\varphi_i(x)\rangle$.

Adding up all the segment volumes in x, $x + dx$ and requiring that the sum of all the contributions is equal to the total volume of this layer, Adx, (i.e., requiring uniform hydrocarbon density) we find, for a symmetric bilayer,

$$\sum_i N_i \sum_{\alpha_i} P(\alpha_i)[\varphi(x;\alpha_i) + \varphi(-x;\alpha_i)] = A \quad (2)$$

for all $-d/2 \le x \le d/2$. Or, defining $X_i = N_i/\sum N_i = N_i/N$ as the mol fraction of i chains in the bilayer, we find

$$\sum_i X_i \sum_{\alpha_i} P(\alpha_i)[\varphi(x;\alpha_i) + \varphi(-x;\alpha_i)] = \sum_i X_i[\langle\varphi_i(x)\rangle + \langle\varphi_i(-x)\rangle] = a \quad (3)$$

where $a = A/N$ is the average area per chain (originating from either the upper or the lower interface). Note that for bilayers composed of single chain amphiphiles a is also the area per headgroup at the hydrocarbon-water interface. For doubly chained phospholipid bilayers the average area per headgroup (or per molecule) is $2a$.

When Eq. 1 is substituted into Eq. 3 we obtain an integral equation for $\pi(x)$. A convenient procedure for solving this equation is to divide the hydrophobic region into, e.g., $2L$ parallel layers of thickness $\Delta x = d/2L$, thus obtaining $2L$-coupled nonlinear equations for the $\pi(x_\ell)$, $x_\ell = \pm\ell\Delta x$ ($\ell = 1, 2, \cdots, L$), which can be solved by standard numerical procedures. The $\varphi(x_\ell;\alpha_i)$ and $\epsilon(\alpha_i)$ appear as input data in these equations. To this end we generate many chain conformations α_i and classify them according to their $\epsilon(\alpha_i)$ and $\varphi(x_\ell;\alpha_i)$. For chains composed of up to ~20 segments one can enumerate all possible bond sequences as well as many combinations Ω, x_0 of overall chain orientations and headgroup altitudes (typically we sample ~40). The headgroup positions x_0 are uniformly sampled within a narrow range δ at both interfaces (we generally take $\delta \sim$ 2–5 Å). However, the final distribution of headgroup positions, $P(x_0)$, is determined by the solutions of the packing constraints (Eq. 3), i.e. by $P(\alpha)$. In general $P(x_0)$ is nearly a gaussian distribution whose width, $\sigma_x = (\langle x_0^2\rangle - \langle x_0\rangle^2)^{1/2}$, is less then δ (typically ~1 Å); see DOPC Bilayers: Adding Double Bonds, below.

For simple, saturated alkyl chains the rotational isomeric state (RIS) model (Flory, 1969) provides a faithful representation of the allowed conformations. For a chain of the type $—(CH_2)_{n-1}—CH_3$ the number of possible (*trans/gauche*) sequences is 3^{n-1}. This number includes self-intersecting conformations (e.g., those involving adjacent bonds in *gauche+/gauche−* states), which are discarded from the calculations. For more complex chains such as those of POPC, an extended RIS model (Flory, 1969) accounting also for —C=C—C— segments is used to generate the possible bond conformations. See Appendix for more details.

From Eq. 3 it is clear that the lateral pressure profile, $\pi(x)$, depends on the membrane composition $\{X_i\}$, and on the value of a. A qualitative interpretation of the physical significance of $\pi(x)$ can be given as follows. Consider a "free", i.e., an isolated ("unperturbed") chain with no neighbors around, and let $\langle\varphi(x)\rangle_f\, dx$ denote the average volume occupied by this chain at $x,x + dx$. (For the free chain $\pi(x) \equiv 0$). Now consider a chain packed in a bilayer, for which we have $\langle\varphi(x)\rangle = a$. If $\langle\varphi(x)\rangle_f > a$ the free chain must be laterally compressed to satisfy the packing constraint $\langle\varphi(x)\rangle = a$. $\pi(x)$, which increases with $\langle\varphi(x)\rangle_f - a$, is the local lateral stress on the chain necessary to satisfy the packing constraint. Thus, generally, as a decreases $\langle\pi(x)\rangle$ increases, reflecting the reduced conformational freedom of the chains associated with the tighter lateral packing. (As a decreases the chains are farther stretched out along the normal to the membrane. In particular, when a decreases to its lowest possible value, ~20 Å^2, the predominant α of saturated alkyl chains is an all-*trans* conformation oriented along the normal of the membrane). A typical $\pi(x)$ profile is schematically illustrated in Fig. 1.

After evaluating the $\pi(x)$, and hence the $P(\alpha_i)$, we can calculate any desirable conformational property. For instance, the average position $\langle\vec{r}_k^{\,i}\rangle$ of the segment k of a chain of type i: $\langle\vec{r}_k^{\,i}\rangle = \sum_{\alpha_i} P(\alpha_i)\vec{r}_k(\alpha_i)$. More generally, using $x_k(\alpha_i)$, $y_k(\alpha_i)$, $z_k(\alpha_i)$ to denote the coordinates of this segment for a chain in conformation α_i, the mth moment of, e.g., the x_k coordinate, is given by

$$\langle(x_k^i)^m\rangle = \sum_{\alpha_i} P(\alpha_i)[x_k(\alpha_i)]^m \qquad (4)$$

For instance, $\sigma_x = (\langle(x_k^i)^2\rangle - \langle x_k^i\rangle^2)^{1/2}$, the root-mean-square deviation of x_k^i, measures the width of the spatial distribution of the segment along the normal of the membrane (see Results and Analysis). Another measurable quantity of interest is the orientational order parameter of a given bond k (e.g., a particular C—H or a C—C bond) of the lipid acyl chain, namely

$$S_k^i = \sum_{\alpha_i} P(\alpha_i)[3\cos^2\theta_k(\alpha_i) - 1]/2 \qquad (5)$$

where $\theta_k(\alpha_i)$ is the angle between the kth bond and the normal of the membrane, when the chain is in conformation α_i.

Thermodynamic quantities can also be calculated using the $P(\alpha_i)$. In particular, the conformational Helmholtz free energy of the membrane is given by

$$F = 2\sum_i N_i\left[\sum_{\alpha_i} P(\alpha_i)\epsilon(\alpha_i) + kT\sum_{\alpha_i} P(\alpha_i)\ln P(\alpha_i)\right] \qquad (6)$$

where it should be remembered that we consider a portion of a bilayer of area A containing $2N_1$ molecules of type 1, $2N_2$ of type 2, etc. The first sum in the square brackets, $\langle\epsilon_i\rangle = \sum P(\alpha_i)\epsilon(\alpha_i)$ is the average internal (*trans/gauche*) energy of chain i. The second sum $-Ts = kT\sum P(\alpha_i)\ln P(\alpha_i)$ is its entropy. Both $\langle\epsilon\rangle$ and s are evaluated in the mean-field approximation, inasmuch as we use the singlet distribution rather than the many-chain distribution. A mixing entropy term $2\sum N_i \ln X_i$ should be added to Eq. 6 if the membrane contains more than one lipid component. Of course we do not include a mixing entropy term when treating a pure bilayer composed of a single lipid with two different (linked) hydrocarbon chains.

We close this section with a remark on the derivation of the $P(\alpha_i)$, as given by Eq. 1. If we regard F in Eq. 6 as a functional of the $\{P(\alpha_i)\}$, then, as is common in statistical thermodynamic variational derivations, the "true" (or "best") probability distribution function of the system is the one that minimizes F subject to whichever constraints $P(\alpha_i)$ must fulfill. In our case the only relevant constraints (apart from normalization $\sum_{\alpha_i} P(\alpha_i) = 1$) are the packing constraints, Eq. 3. Indeed, the probability distributions that minimize Eq. 6 subject to Eq. 3 are those given by Eq. 1 with the $\pi(x)$ serving as the Lagrange multipliers conjugate to the packing constraints. Note that the same lateral pressure profile $\pi(x)$ appears in all the $P(\alpha_i)$.

RESULTS AND ANALYSIS

In this section we present numerical calculations for the conformational properties of the lipid chains constituting the hydrophobic cores of DPPC, DOPC, and POPC bilayers, and compare them with available experimental and computer simulation studies. The chemical structure of these lipids is of the general form R_1-$\mathcal{H}$-R_2 with $\mathcal{H}$ representing the headgroup, and R_1 and R_2 are the two hydrocarbon chains. In all these cases the headgroup has the structure $\mathcal{H}$ = (PC)—CH_2—CH[(C_aOO)—]—CH_2[(C_bOO)—] with PC = $(CH_3)_3N(CH_2)_2$—$O(PO_2)O$— denoting the phosphatidylcholine group, and C_a and C_b are the carbonyl atoms from which the two lipid chains R_1 and R_2 originate. R_1 and R_2 are either the fully saturated palmitoyl R = —$(CH_2)_{14}$—CH_3 ("C_{15}") chain, or the monounsaturated oleoyl R = —$(CH_2)_7$—(CH=CH)—$(CH_2)_7$—CH_3 ("C_{17}") chain. Following Wiener and White (1992*a*,*b*) we shall assume that the average position of the carbonyl groups marks the boundary between the hydrocarbon region and the aqueous interfacial region containing the headgroups. We shall also assume that in the fluid phase of the bilayer the interactions between hydrocarbon chains (R_1, R_2) originating from a common headgroup are the same as those between chains belonging to different headgroups. Although the two carbonyl groups of the lipids are positionally nonequivalent

in both the gel and fluid ("liquid-crystalline") phases (Elder et al., 1977; Büldt et al., 1978; Seelig and Waespe-Šarčević, 1978; Seelig and Seelig, 1980; Hauser et al., 1981), it has been argued that the time-averaged thermal motions in the fluid phase partly obscure the differences between the two chains (Wiener and White, 1992*b*; Smith et al., 1992; Hübner et al., 1994). Accordingly, in the calculations described below, the lipid bilayer has been treated as an equimolar (random) mixture of $P—R_1$ and $P—R_2$ chains, with P symbolizing the carbonyl groups.

As explained in the previous section, the segments of the R_1 and R_2 chains are confined to the hydrophobic region of the bilayer (of thickness d) in which they are packed so as to ensure uniform segment density. Recall that in generating the possible chain conformations we allow the (centers of the) headgroups P to fluctuate (normal to the membrane plane) within a narrow interval of width δ at the interface of the membrane. The actual width of the distribution of the headgroup, $\sigma_x = (\langle x_0^2 \rangle - \langle x_0^2 \rangle)^{1/2}$, is smaller than δ (see also DOPC Bilayers: Adding Double Bonds). The first two to three segments of the chains are also allowed to protrude into this region, thus accounting for some "roughness" fluctuations of the hydrophobic core.

DPPC bilayers

We model the hydrophobic core of the DPPC bilayer as a single component system composed of C_{15} chains ($R_1 = R_2 = —(CH_2)_{14}—CH_3$). The chain packing characteristics were calculated as explained above, at temperature $T = 333$ K. At this temperature the bilayer is in its fluid state. The calculations were performed for four different average headgroup areas (per single chain): $a = 25.5$, 26.6, 29.6, and 31.3 Å^2, which correspond to a hydrophobic bilayer thickness (i.e., transbilayer separation of the carbonyl groups) of 33.9, 32.5, 29.2, and 27.6 Å, respectively. The values of the area per headgroup were chosen so as to correspond to the values estimated by S. Kõnig et al. (1992) in their study of DPPC bilayers using incoherent quasi-elastic neutron scattering.

The motions of the methylene and methyl chain segments become less restricted the farther they are from the glycerol backbone (Kõnig et al., 1992; Wiener and White, 1992b; Elder et al., 1977). The root-mean-square deviations of chain segments around their equilibrium positions can be easily calculated using the singlet probability of chain conformations, $P(\alpha)$. We shall refer to them as "segment fluctuations" (following Kõnig et al., 1992). Yet it should be emphasized that they do not reflect monomer density fluctuations within the membrane, which remains uniform throughout.

The segment motion in the plane perpendicular to the membrane normal ("in-plane motion") can be described in terms of the in-plane root-mean-square deviation of the segment center ("in-plane fluctuation"): $\sigma_{yz} = (\langle y_n^2 \rangle + \langle z_n^2 \rangle)^{1/2}$ (the x axis is parallel to the bilayer normal), where the averaging is over all chain conformations. Notice that, because the in-plane motion is isotropic in the liquid phase, $\langle y_n \rangle = \langle z_n \rangle = 0$. Plotted in Fig. 2 are the in-plane fluctuation values of the chain segments for the four different average headgroup areas. For each a the calculated values were fitted by a straight line. Clearly, the fit is quite good, meaning that the in-plane fluctuations of the saturated chain segments grow approximately linearly with their distance from the glycerol headgroup. The fluctuations range from ~0.9 Å near the glycerol backbone to 5.1–7.4 Å at the terminal methyl group. The fluctuations of a given segment increase with the average area per headgroup, a result verified experimentally. This is expected, given that interchain repulsion increases with the headgroup lateral packing density. The range of σ_{yz}, 0.9–6.9 Å, found for $a = 29.6$ Å^2 agrees well with the range 0.6–7.0 Å reported by S. Kõnig et al. (1992).

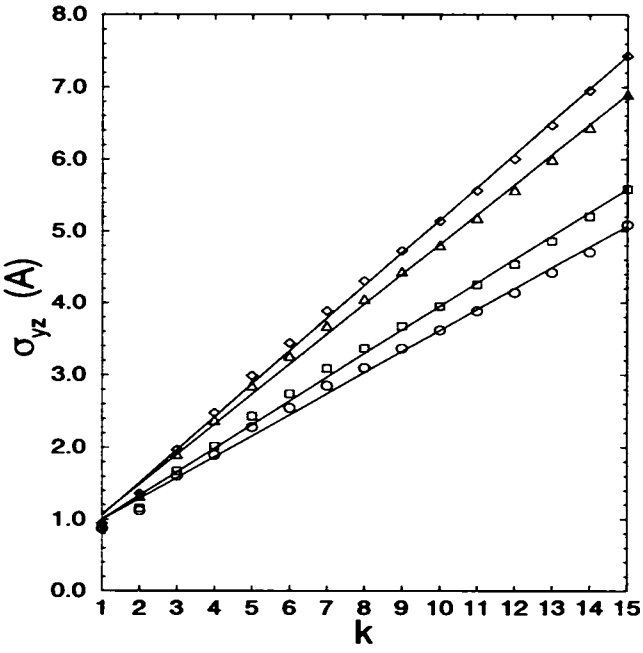

FIGURE 2 Calculated root-mean-square in-plane fluctuations of the carbon atoms, $k = 1, \cdots, 15$, along the hydrocarbon chains of DPPC. ○, □, △, and ◇ correspond, respectively, to an average cross-sectional area/chain of $a = 25.5$, 26.6, 29.6, 31.3 Å^2. The straight lines are linear fits.

The segment root-mean-square deviations parallel to the membrane normal ("out-of-plane fluctuation"), $\sigma_x = (\langle x_n^2 \rangle - \langle x_n \rangle^2)^{1/2}$, are plotted in Fig. 3 for the different a values. As can be seen, the out-of-plane fluctuations of the segments do not vary linearly with the carbon number along the chain, although they do increase monotonically. Also, the range of out-of-plane fluctuations is smaller than that of the in-plane motion: 0.6 Å to 2.3–2.9 Å. Qualitatively, this finding is supported by the observation of Kõnig et al. (1992) that the lipid chains show higher mobility in the plane of the membrane than that perpendicular to this plane. However, the absolute values of the experimental σ_x are significantly lower than the calculated ones. For comparison, Kõnig et al. (1992) report a range of 0.5–6.0 Å for headgroup area of 29.6 Å^2 (assuming a linear fit) whereas we calculate a range of 0.6–2.7 Å. Note, however, that "global" fluctuations caused by the slow, thermally excited membrane undulations that may contribute to the experimental signals are not accounted for by our calculations.

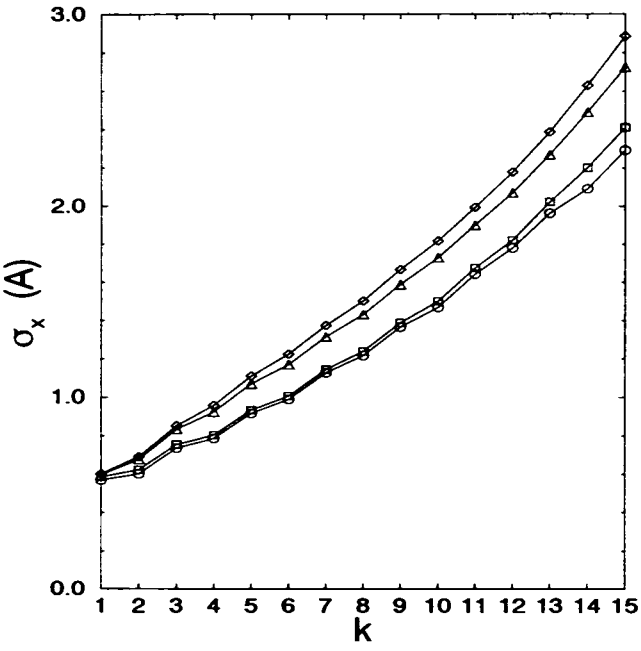

FIGURE 3 Calculated root-mean-square out-of-plane fluctuations (along the normal to the membrane plane) of the carbon atoms, $k = 1, \cdots, 15$, along the hydrocarbon chains of DPPC. ○, □, △, and ◇ correspond, respectively, to an average cross-sectional area/chain of a = 25.5, 26.6, 29.6, and 31.3 Å^2.

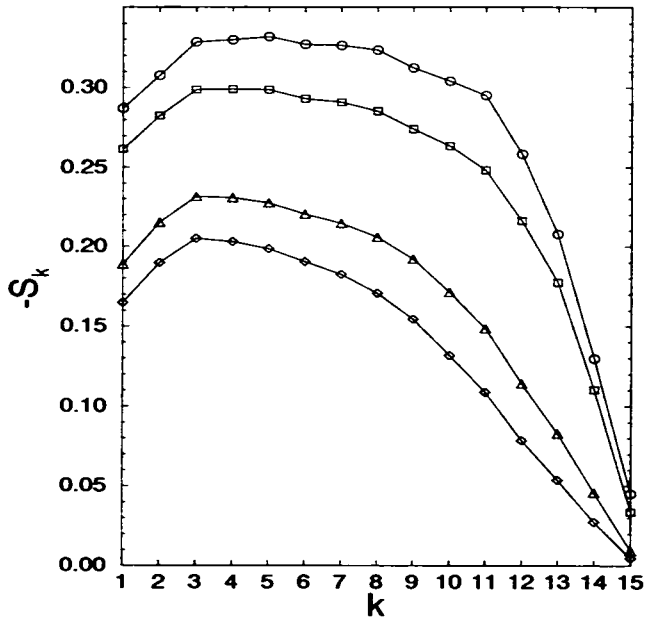

FIGURE 4 Calculated orientational order parameters of the C_k—H bonds along the hydrocarbon chains of DPPC. ○, □, △, and ◇ correspond, respectively, to an average cross-sectional area/chain of a = 25.5, 26.6, 29.6, 31.3Å^2.

Generally, our calculations lend support to the model proposed by König et al. (1992) for the local lipid motion as a superposition of in- and out-of-plane diffusion of the methylene groups inside a restricted volume, which they assume to be a cylinder. To account for the experimental observation of increasing flexibility along the hydrocarbon chain they assume a distribution of radii/heights between two limiting values, the distribution taken to be linear for simplicity. The fact that our results are similar to those found by König et al. (1992) by incoherent quasi-elastic neutron scattering suggests that the local average dynamic picture of the bilayer that they measure is similar to our theoretical static one.

The notion of a flexibility gradient (i.e., increased lateral mobility along the chain) is further supported by the calculated C—H bond orientational order parameter profiles as shown in Fig. 4 for the four different a values. The fraction of *gauche* conformers increases with distance from the headgroup, resulting in lower bond orientational order parameters. The smaller a is, i.e., the thicker the membrane, the more the chains must stretch out, resulting in higher orientational ordering.

DOPC bilayers: adding double bonds

The results presented in this section are for a bilayer composed of P —$(CH_2)_7$—$(CH)_2$—$(CH_2)_7$—CH_3 ("C_{17}") monounsaturated single chains, with the double bond in the *cis* conformation, representing the DOPC double-chain lipids: $\mathcal{H}$—[—$(CH_2)_7$—$(CH)_2$—$(CH_2)_7$—CH_3]$_2$. The calculation was performed for a fluid bilayer at temperature T = 296 K and for an average area/chain a = 29.7 Å^2, (59.4 Å^2/headgroup), which corresponds to a hydrophobic bilayer thickness of 32.0 Å. These values are the same as those measured by Wiener and White (1992b) in their study of DOPC membranes by joint refinement of x-ray and neutron diffraction data.

Fig. 5 shows the distribution of methylene (—CH_2—) groups, double-bonded methyne carbons (—CH=) and terminal methyl (CH_3) segments as a function of the distance from the center of the bilayer, for chains originating from both interfaces. More precisely, the figure shows the volume density distributions, i.e., the contribution (volume/unit length) of the various segments to the volume of the bilayer; these are the $\langle\varphi_s(x)\rangle$ defined in the Theory section. Also plotted is the total segment volume density. The segment densities of each chain are normalized to the total chain volume, in units of $v = v_{CH2}$ (i.e., $\sum_s \langle\varphi_s(x)\rangle\, dx = v/v$ where v is the volume of the chain and v = 27 Å^3). In these units v_{CH3} = 2, v_{CH} = 0.8 and the total volume of the —$(CH_2)_7$—$(CH)_2$—$(CH_2)_7$—CH_3 chain is 14 + 2 × 0.8 + 2 = 17.6. The figure reveals some interdigitation (midplane crossings) of the methylene and methyl groups of chains originating from opposite interfaces. On the other hand, the double-bond distributions do not overlap. Notice that the total density is constant throughout the bilayer, as we assume.

Fig. 6 shows the sum of contributions from chains originating from both interfaces to the segment number density distributions; these are designated by the $\langle\psi_s(x)\rangle$ defined in the Theory section (number of segments/unit length along the bilayer normal). Also shown, for comparison, are the experimental distributions reported by Wiener and White (1992a,b). Both distributions are normalized to the total num-

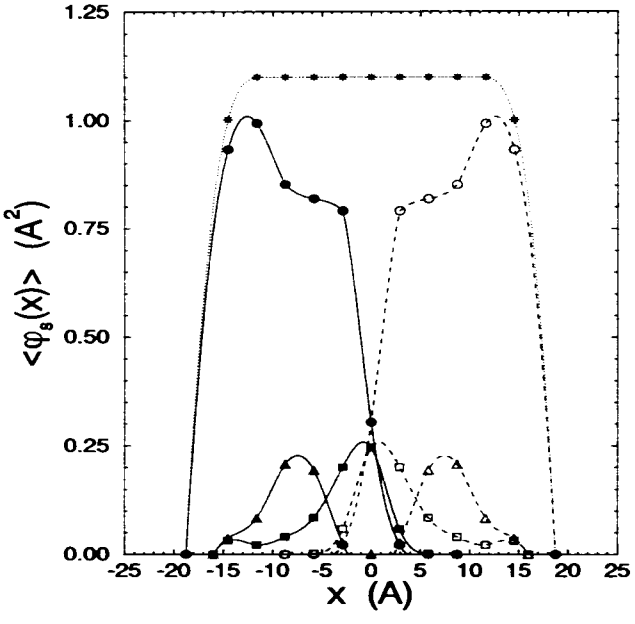

FIGURE 5 Segment volume distributions across a DOPC bilayer, as a function of the distance from the midplane of the bilayer. Solid and open symbols correspond to chains originating from opposite interfaces. Circles represent the distribution of CH_2 groups, the squares correspond to the terminal CH_3 groups and the triangles represent the CH=CH groups. The asterisks correspond to the sum of all segment densities. The lines are drawn only for clarity.

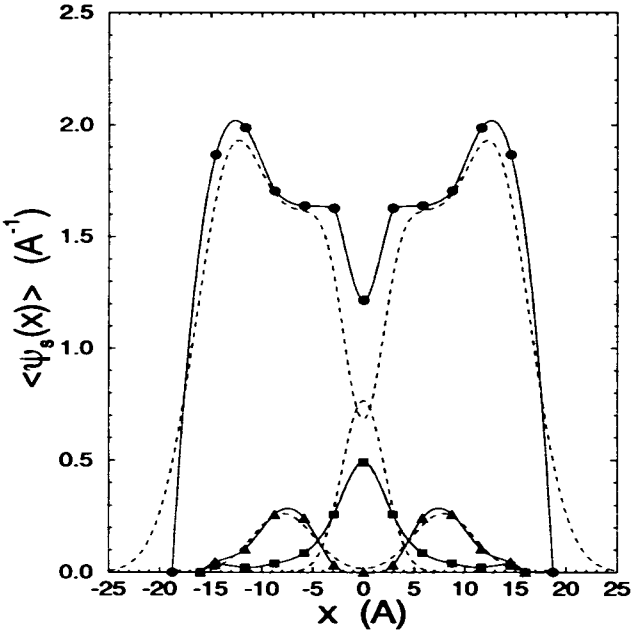

FIGURE 6 Segment (number) distributions across a DOPC bilayer. The solid symbols represent the sum of contributions from chains originating from opposite interfaces, calculated by the mean-field theory. ○, □, and △ represent, respectively, the calculated number densities of CH_2, CH_3, and CH=CH groups. The solid lines connecting the calculated points are drawn only for clarity. The dashed lines are the experimental results of Wiener and White (1992b).

ber of segments of two molecules (two double chains), i.e., 64; (methyl and methylene groups count as one segment each; a double bond counts as one segment). Overall, the agreement between the experimental and calculated results is quite good. The figure shows that the contribution of the methyl groups is peaked at the bilayer center where the contribution of the methylenes is minimal. The distribution of the terminal methyl groups and of the double bonds are approximately gaussian, as assumed by Wiener and White (1992a,b). The peaks of the calculated methyl and double-bond distributions occur at the same positions as the experimental ones, and their widths (at half maximum) are also about the same. We also note that 1), the calculated methyl group distributions corresponding to chains originating from opposite interfaces largely overlap, and are characterized by relatively long tails; and 2), the calculated double-bond distributions do not overlap. On the other hand, Wiener and White (1992b) find some overlap between the double bond distributions, whereas their (total) methyl distribution is relatively sharply peaked at the midplane of the bilayer. They interpret the sharp methyl distribution as indicative of chain tethering. It should be noted, however, that this conclusion is at variance with the notion that, generally, the motions of the hydrocarbon chain segments become less restricted the farther they are from the glycerol backbone, a fact supported by various experimental results (König et al., 1992; Wiener and White, 1992b; Elder et al., 1977) as well as by several theoretical studies (Heller et al., 1993; De Loof et al., 1991; Gruen and de Lacey, 1984). See also the discussion of segment distributions in POPC Bilayers: Chain Mixtures, below. Also, the peak in the experimental methyl distribution correlates with a (small) peak in the hydrophobic segment distribution across the bilayer, implying a not entirely uniform density profile, as opposed to our assumption. Wiener and White attribute this finding to experimental uncertainties.

As noted in the beginning of this section we treat the headgroups as structureless ("point") particles, and in generating the possible chain conformations their positions are sampled (uniformly) within an interval δ normal to the interface. The actual distribution of headgroup positions $P(x_0)$ is dictated by the requirement for uniform hydrocarbon density within the hydrophobic core, and it is not uniform within δ. For the calculation shown in Fig. 6 we have used $\delta = 5.5$ Å, but $P(x_0)$ is nearly gaussian with $\sigma_x = (\langle x_0^2 \rangle - \langle x_0 \rangle^2)^{1/2} = 1.1$ Å. (The average separation between the carbonyl groups on opposite interfaces is $d = 2\langle x_0 \rangle \simeq 31$ Å). Of course, we could allow for larger σ_x, as well as relax the requirement for uniform hydrocarbon density to a region somewhat smaller than the hydrophobic thickness d of the bilayer. This could also improve the fit between the experimental CH_2 density profile and the calculated one; the latter is considerably sharper as we see in Fig. 6. Yet considering our approximate treatment of the headgroup geometry and the lack of reliable headgroup-water interaction potentials (which should be included if one allows for large headgroup protrusions), we feel that such ramifications are not warranted at this stage, and would only add adjustable parameters to our simple model. Furthermore, it should be noted that several other factors

could possibly contribute to the larger width of the experimental CH_2 profile as compared with the calculated one. Apart from some inherent experimental uncertainties, one possible contribution could be bilayer thermal undulations (Wiener and White, 1992b). Note also that the widths of the experimental distributions (of both headgroup and hydrocarbon groups) involve a convolution of the van der Waals hard core radius of the fragments and the gaussian envelope of the thermal motion of its center. On the other hand, our calculations involve only the latter factor. Finally it should be noted that protrusion of the CH_2 groups to ~3 Å beyond the experimental carbonyl distributions (see Fig. 6), must be caused by distant methylenes along the chain, given that the position of the first carbon is constrained by the carbonyl-carbon bond not to exceed 1.54 Å. This behavior is not seen in MD simulations (on POPC) performed by Heller et al. (1993); see next subsection for a discussion of these results.

POPC bilayers: chain mixtures

The POPC bilayer is modeled as an equimolar mixture of palmitoyl chains, P—$(CH_2)_{14}$—CH_3, and *cis* oleoyl chains P—$(CH_2)_7$—(CH=CH)—$(CH_2)_7$—CH_3. The calculation was performed for a fluid bilayer at temperature $T = 300$ K, for an average total area/molecule (with one oleoyl chain and one palmitoyl chain) of 60.5 Å^2, which corresponds to a hydrophobic bilayer thickness of 30.0 Å. Recently Heller et al. (1993) presented results of an MD simulation of a POPC lipid bilayer composed of 200 molecules in the gel and liquid phases. For the liquid phase simulation they report an area/headgroup of 65.5 Å^2 and a transbilayer separation between the carbonyl groups of 29 Å. Notice that the calculated area/headgroup is based on the assumed total chain volume and therefore might vary between different calculations. Thus a comparison of different results should, in principle and if possible, be done for membranes of the same total hydrophobic thickness, i.e., equal transbilayer headgroup separation. The calculations presented in this section were performed in order to compare the mean-field results with those of MD simulations (Heller et al., 1993).

In Fig. 7 *a* we show the total segment (number) densities calculated according to our mean-field theory. Plotted are the sums of contributions to the density of CH_2, CH_3, and CH segments from two oleoyl chains, originating at opposite interfaces. Also shown is the sum of CH_2 and CH_3 segment densities from the two-palmitoyl chains. For clarity, the calculated points were fitted by a smooth curve using a cubic spline. For comparison the corresponding distributions calculated by MD simulations (Heller et al., 1993) are plotted in Fig. 7 *b*. Notice that only the sum of both the terminal methyl distributions of the palmitoyl and oleoyl chains are shown in Fig. 7 *b*. The distributions in Fig. 7, *a* and *b*, of each chain, are normalized to the total number of segments of two chains as follows: $A_{CH2,palmitoyl} = 28.0$, $A_{CH3,palmitoyl} = 2.0$, $A_{CH2,oleoyl} = 28.0$, $A_{CH3,oleoyl} = 2.0$ and $A_{CH,oleoyl} = 4.0$, where A symbolizes the total area under the respective distribution.

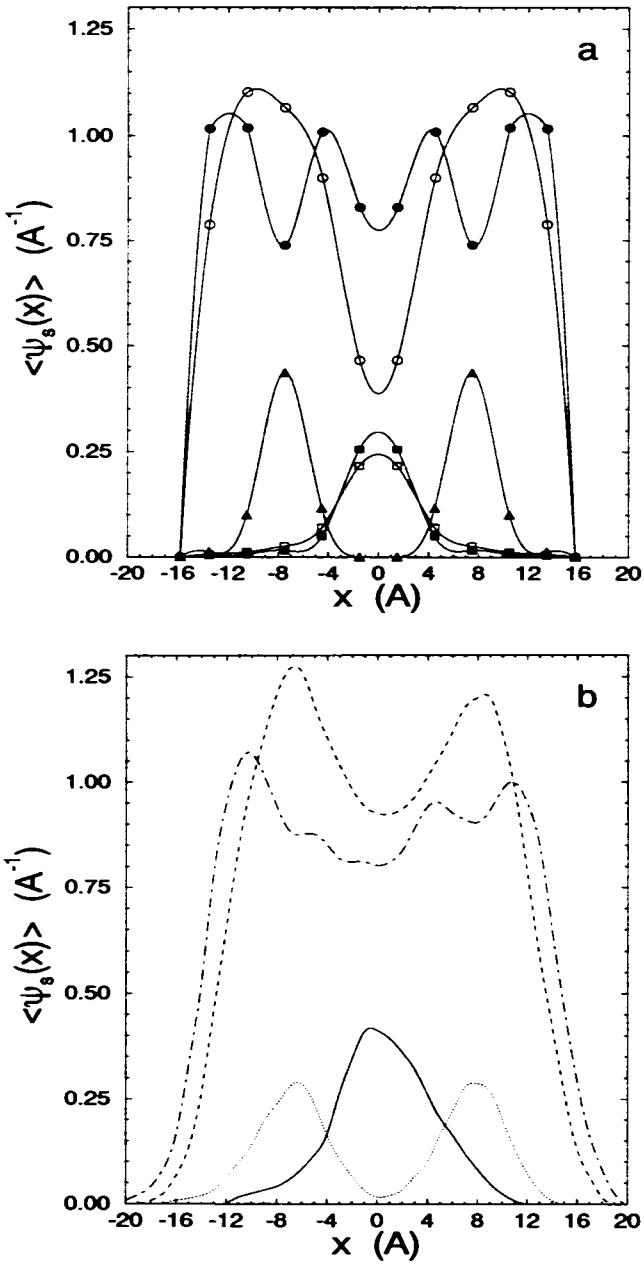

FIGURE 7 (*a*) Segment (number) distributions across a POPC bilayer. The solid and open symbols correspond, respectively, to the calculated sum of contributions from the oleoyl and palmitoyl chains originating from opposite interfaces. Circles, squares and triangles represent, respectively, the calculated number densities of CH_2, CH_3, and CH=CH groups. The solid lines connecting the calculated points are drawn only for clarity. (*b*) The corresponding MD distributions of Heller et al. (1993). The dashed, dot-dashed, dotted, and solid lines are, respectively, the palmitoyl CH_2, oleoyl CH_2, oleoyl CH=CH, and total (palmitoyl and oleoyl) CH_3 distributions.

Comparing the density profiles in Fig. 7, *a* and *b*, we note their similar shapes and peak positions. The major difference is in the distribution of the CH_2 segments of the palmitoyl, which in the MD simulations is larger than ours around the midplane of the bilayer. The MD distributions are also more spread out than ours, given that in our calculations we assume a rather well defined ("compact") hydrophobic core and relatively small headgroup fluctuations. The small number of

palmitoyl methylene groups in the bilayer center in Fig. 7 *a* is a result of the presence of the longer (unsaturated oleoyl chain) methylene groups and the terminal methyl groups there. An obvious result of the packing requirement in the mean-field theory is the fact that the distribution of CH_3 groups of the longer (oleoyl) chain is more concentrated in the center of the bilayer. Unlike in the MD results, our calculations show no overlap between the distributions of double-bond segments belonging to chains originating from opposite interfaces. (See also discussion of Fig. 10, below). For a membrane with a smaller hydrocarbon thickness interdigitation of this sort would be seen. Finally, we note that in our calculations the methylenes of the oleoyl do not extend beyond those of the saturated palmitoyl chain, as opposed to the behavior seen in the MD simulation. This is because of the fact that in our calculations we have treated the headgroups as simple rigid atoms, ignoring their internal structure and conformational degrees of freedom. This shortcoming could, in principle, be remedied in future calculations.

Fig. 8 shows the orientational bond order parameter profiles of CH bonds along the palmitoyl (sn1) and oleoyl (sn2) chains of POPC. Also plotted are the MD values of Heller et al. (1993) and the experimental results of Seelig and Waespe-Šarčević (1978), for the two chains of POPC at a temperature of 300 K. The different profiles cannot be expected to be identical, as the experimental hydrophobic bilayer thickness was not measured in the experiments, and therefore might be different from the value of 30.0 Å assumed in our calculations, and given that the MD simulation time was relatively short (56 ps). Furthermore our RIS model for chain conformations is not identical to the model used in the MD simulations. Nevertheless, the basic features of the results obtained by our mean-field calculations are quite similar to those observed experimentally and in the MD simulations. The order parameter profiles obtained in the MD simulations lie below ours for carbons close to the headgroup and above ours for the end carbons. Heller et al. (1993) note that the profiles computed toward the end of the simulation period (longer simulation time) progressively approach the experimental values. The MD odd-even effect at the beginning of the oleoyl chain as well as the low experimental and MD values are probably due to the fact that the carbonyl—C(1) bond in the *sn*2 chain is not aligned parallel to the bilayer normal (Seelig and Seelig, 1980; Hauser et al., 1981; Seelig and Waespe-Šarčević, 1978), whereas in our calculation the average bond orientation is parallel to the bilayer normal because we do not calculate the exact headgroup conformations.

The molecular order parameter we calculate (profile not shown) for the C=C bond is 0.37, and −0.067 for the following bond. These are in good agreement with the MD values of 0.40 and −0.063, respectively, as well as with the experimental value of 0.37 for the double bond as reported by Seelig and Waespe-Šarčević (1978). We also find that the average angle between the double bond and the bilayer normal is 43.92°, in reasonable agreement with the average value of 38.43° determined by Heller et al. (1993), whereas

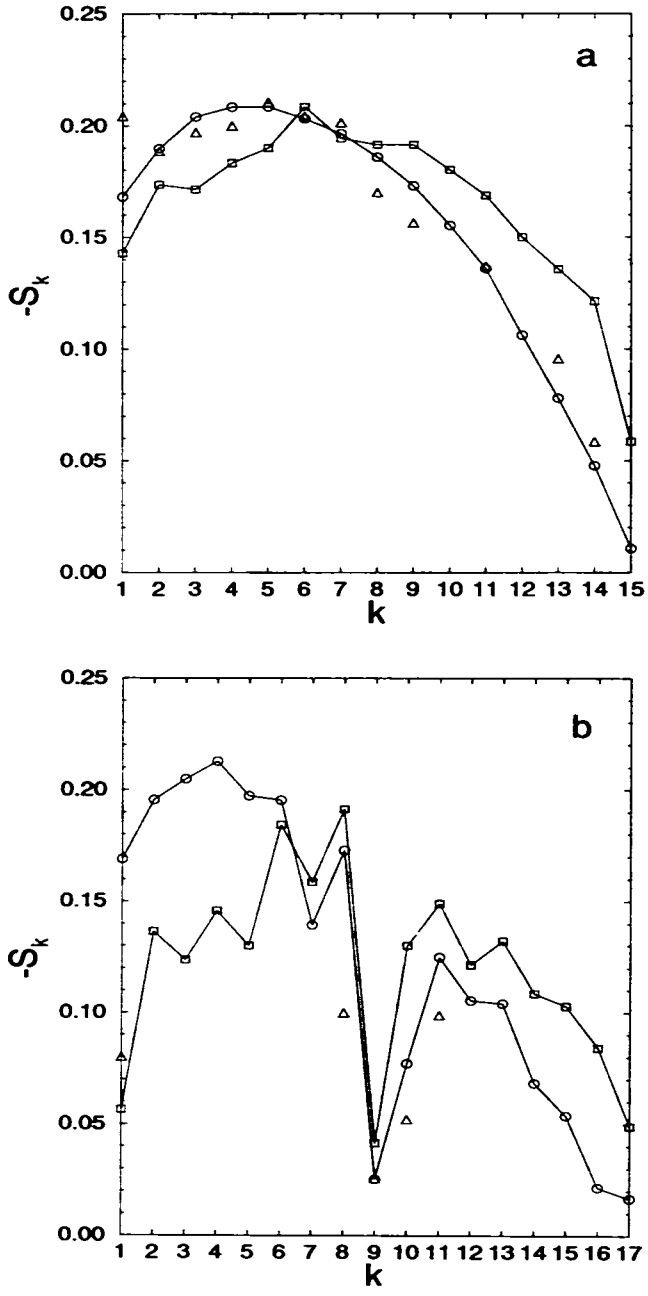

FIGURE 8 Orientational order parameters of the C_k—H bonds along the palmitoyl (*a*) and oleoyl (*b*) chains of POPC. ○, □, and △ correspond, respectively, to results calculated by the mean-field theory and MD results of Heller et al. (1993) and the experimental results of Seelig and Waespe-Šarčević (1978).

Seelig and Waespe-Šarčević (1978) estimate a value of 9°. As noted by Heller et al. (1993), for a perfect all-*trans* chain (except for the *cis*-double bond), with the segments from C(1) to C(7) perfectly aligned along the bilayer normal as in the gel phase, the angle of the double bond with the bilayer normal would be 26°, (according to the RIS model the angle would be 21°; see Appendix). This indicates considerable motional freedom of the hydrocarbon tail (compared with the gel phase) and that the low-order parameter for the second carbon atom of the double bond is a geometrical as well as

an ordinary liquid-phase fluctuation effect (Seelig and Waespe-Šarčević, 1978). For the average angle of the bond C(9)—C(10) we find 67.84°, which compares well with the MD value of 65.55°. As noted by Heller et al. (1993) this is smaller than the value of 86° (76° according to the RIS model) for a perfect all-*trans* geometry, a result of the realigning of the tail segments C(10)—C(17) along the bilayer normal caused by packing requirements. The low order parameter that we find for C(10) (in agreement with the experimental result but at variance with the MD result) therefore is caused by a geometrical effect as well as a packing requirement. An examination of the in-plane and out-of-plane fluctuations of the different carbons shows that these effects are quite strict and result in relatively low fluctuation values for the oleoyl C(10); see the discussion after Fig. 10, below.

Comparison of different chains

The conformational properties, e.g., the orientational order parameters, of the chains composing a "pure" (single chain component) bilayer depend, primarily, on the average cross-sectional area a per chain (Ben-Shaul and Gelbart, 1994). Namely, the order parameters decrease as a increases, or equivalently, as the bilayer thickness $d = 2v/a$ decreases, with v denoting the volume of the chain. This is the behavior expected, for instance, in a DPPC or a DOPC bilayer whose hydrophobic cores are composed of palmitoyl and oleoyl chains, respectively. On the other hand, in mixed bilayers the conformational properties may also depend on chain composition. It is thus of interest to compare the packing characteristics of the oleoyl and palmitoyl chains in a POPC bilayer, which we have treated as an equimolar mixture of the two types of chains, to those in the "pure" DOPC and DPPC bilayers. Thus, in Fig. 9 we show bond orientational parameter profiles of the oleoyl and palmitoyl chains packed in DPPC, DOPC, and POPC bilayers, all of the same thickness $d = 30$ Å and at the same temperature $T = 300$ K. Using a_p and a_o to denote the average cross-sectional area/chain in the DPPC and DOPC bilayers we have $a_p = 2v_p/d = 28.8$ Å^2 and $a_o = 2v_o/d = 31.7$ Å^2, with v_p and v_o denoting the volume of the palmitoyl and oleoyl chain, respectively. The average area/molecule (double chain) in the POPC bilayer is therefore $a = 2(v_p + v_o)/d = 60.5$ Å^2, which is simply the sum of the areas per chain in the pure systems. In other words, on the average, the area per palmitoyl or oleoyl chain is the same in the pure and mixed bilayers.

The results shown in Fig. 9 reveal a significant change in the degree of chain ordering upon mixing. The order parameters of the longer, oleoyl, chains increase, whereas those of the shorter, palmitoyl, chains decrease. This indicates an increase in the free energy (lower entropy, lower flexibility) of the longer chains and an opposite behavior of the shorter ones. Clearly, the sum of these changes amounts to lower free energy in the mixed system (as confirmed by numerical calculations of these quantities). This behavior is in qualitative agreement with a simple scaling argument according to which the free energy/chain varies with the area/chain a via

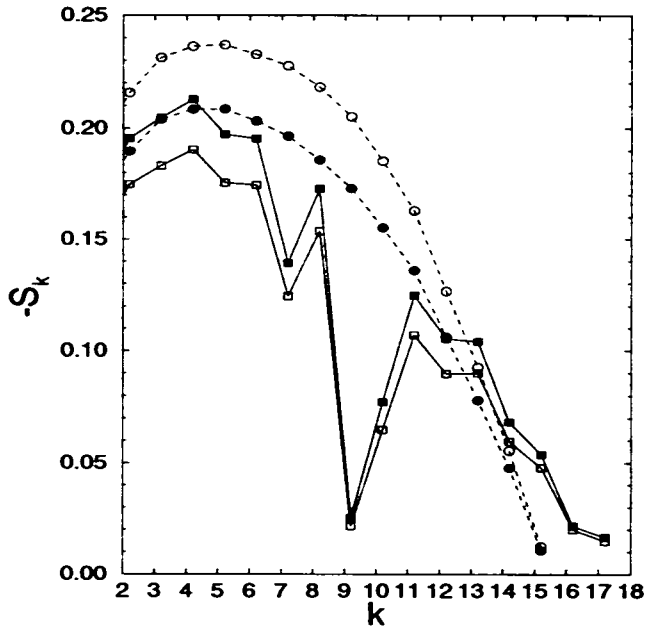

FIGURE 9 Orientational order parameters of the C_k—H bonds along the chains of POPC, DPPC, and DOPC. The solid and open circles correspond, respectively, to the palmitoyl chains of POPC and DPPC. The solid and open squares correspond, respectively, to the oleoyl chains of POPC and DOPC. The average cross-sectional area/chain of the palmitoyl and oleoyl chains are $a = 28.8$ and 31.7 Å^2, respectively.

$f \sim n/a^2$ where n is the chain length (Fattal and Ben-Shaul, 1993; Ben-Shaul, 1994). According to this rule the free energy gain of a stretched chain (small a) when $a \rightarrow a + \delta a$ is larger than the free energy loss associated with stretching a relaxed (large a) chain, $a' \rightarrow a' - \delta a$ ($a' > a$). The behavior displayed in Fig. 9 is also consistent with the results of Seelig and Seelig (1977), who found lower-order parameters for the palmitoyl chains in POPC as compared with DPPC. It should be noted, however, that in their experiments the POPC bilayer has a smaller thickness than that of the DPPC bilayer. According to our calculations the effects would be even stronger for a thinner POPC bilayer.

The similarity of the shapes of the order parameter profiles of a given chain in different environments suggests that the shape is determined by the chemical structure of the chain. The absolute values of the order parameter, however, depend on the membrane composition. Particularly, *cis* unsaturated chains have a disordering effect, whereas saturated chains induce ordering. Finally, a comparison of the two POPC profiles shows that the end of the oleoyl chain is slightly more ordered than that of the palmitoyl because of the realigning effect of the oleoyl C(10)—C(17) segments along the bilayer normal, as discussed above. The similarity of the bond order parameters for the two chains of POPC up to C(4) is a result of our assumption that they originate from similar headgroups, which is, obviously, an approximation.

Fig. 10 shows the root-mean-square deviations of the in-plane and out-of-plane motions of the carbon atoms along the palmitoyl and oleoyl chains. The fluctuations of the chain segments grow with their distance from the glycerol head-

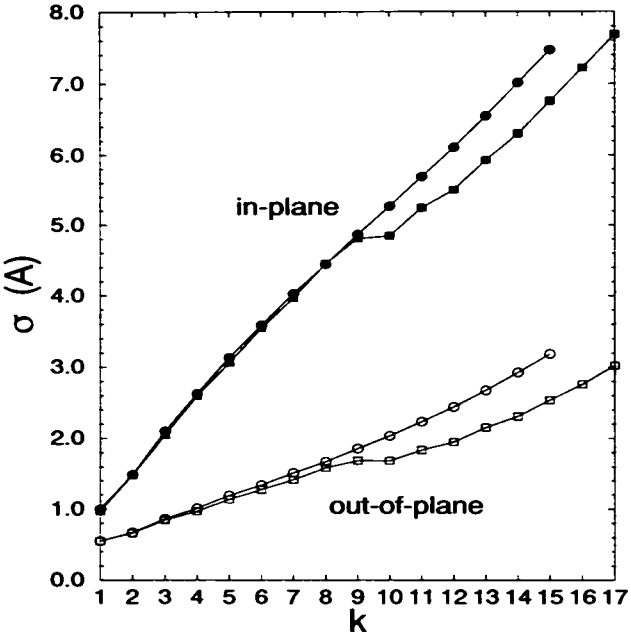

FIGURE 10 Calculated root-mean-square in-plane and out-of-plane fluctuations of the carbon atoms along the palmitoyl and oleoyl chains of POPC. The solid and open symbols correspond, respectively, to in-plane and out-of-plane fluctuations. The circles and squares correspond to the palmitoyl and oleoyl chains, respectively.

group, in agreement with the MD results of Heller et al. (1993) and various experimental results (König et al., 1992; Wiener and White, 1992b; Elder et al., 1977). As noted in the section DPPC Bilayers, above, the amplitudes of out-of-plane fluctuations are smaller than those of in-plane motion. The calculated fluctuation range of a saturated palmitoyl chain in POPC at 300 K is slightly larger than that of a palmitoyl chain in DPPC at 333 K, of equal headgroup area (~29.0 Å), even though the range of the fluctuations is expected to become larger as the temperature is increased (see Figs. 2 and 3). We therefore conclude that the amplitudes of chain segment fluctuations depend primarily on membrane composition and the average cross-sectional area/chain. The presence of the oleoyl chain allows for larger palmitoyl fluctuations, a notion supported by the lowering of the order parameter as discussed in relation to Fig. 9. The fluctuations calculated by Heller et al. (1993) are much smaller than ours (results not shown), although their qualitative findings are similar. The differences may be caused by the relatively short simulation time (46 ps).

From Fig. 10, the fluctuations (both in- and out-of-plane) of the the two oleoyl carbons C(9) and C(10) are practically equal. Thus for the oleoyl carbons C($\geq$10) the fluctuation values are smaller than those of the saturated palmitoyl chain. According to Heller et al. (1993) (results not shown); however, the oleoyl carbons C(8) and C(9) show increased flexibility compared with the saturated chain, carbons C(10) to C(13) have fluctuation values practically equal to those of the saturated chain, and carbons C($\geq$14) have fluctuation values below those of the saturated chain. The assertion by Heller et al. (1993) that the experiments of Wiener and White (1992a,b) support their result that the double bond carbons have increased flexibility, appears lacking: Wiener and White base this conclusion on the fact that their terminal methyl group fluctuates less than the double bond (as discussed in the previous subsection), and this behavior is opposed to both our results and the MD ones. The fact that according to our calculations the fluctuation of the oleoyl C(10) is relatively small and affects the rest of the hydrocarbon tail seems reasonable in view of the realigning of segments C(10) to C(17) along the bilayer normal (caused by the packing requirement), as discussed above. It cannot be ruled out, however, that the MD results reflect a cooperative phenomenon, in which case they cannot be accounted for by our mean-field approach.

CONCLUSION

The main purpose of this paper was to demonstrate that a relatively simple molecular theory can account quite well for many of the important conformational characteristics of lipid chains in membranes. In fact, as discussed elsewhere (Ben-Shaul et al., 1985; Ben-Shaul and Gelbart, 1994), it is not too surprising that a mean-field theory can faithfully reproduce single-chain properties, i.e., properties that are determined by the singlet distribution of chain conformations. Considering the fact that such mean-field calculations are relatively easy to perform, their usefulness for systematic studies of specific systems as well as of general trends, e.g., conformational and/or thermodynamic properties of lipid bilayers of different compositions, temperatures, or curvatures is quite obvious. The major limitation of the approach described here is the assumption of an a priori given (e.g., a sharply defined) hydrocarbon-water interface. To remedy this limitation the electrostatic interactions prevailing in the interfacial (aqueous headgroup) region should be treated in a detailed fashion, comparable to the level we have treated the hydrophobic chain region. Some models that account for the electrostatic interactions (Dill and Stigter, 1988; Stigter and Dill, 1988; Winterhalter and Helfrich, 1992; Ennis, 1992; Andelman, 1994) have been suggested, and it would be of interest to combine them with our chain packing model to obtain a unified (albeit mean-field) molecular theory of lipid bilayers. Clearly, such theories cannot, and are not intended to, substitute detailed computer simulation studies, but rather are intended to supplement them by considering wider ranges of initial conditions and by providing additional qualitative insights into the underlying physics.

APPENDIX: ROTATIONAL ISOMERIC STATES OF LIPID CHAINS

In all the calculations presented in this work the possible conformations of the lipid chains were generated and classified according to the rotational isomeric state model (Flory, 1969). Generally, according to this model every bond along a hydrocarbon chain can be found in one of several states, corresponding to specific rotational angles around the particular bond. More specifically, let C_{k-2}, C_{k-1}, C_k, and C_{k+1} denote four consecutive (methylenic, methylic, or methynic) carbon atoms of the chain, and let us refer to

the vector connecting C_{k-1} and C_k as the kth C—C bond. Then φ_k, the angle of rotation around the kth bond, is the (dihedral) angle between the planes formed by carbons C_{k-2}, C_{k-1}, C_k, and C_{k-1}, C_k, C_{k+1}, respectively. In the rotational isomeric state model φ_k can assume only few special values, corresponding to the local minima of the potential energy. φ_k and other molecular parameters used in our calculations to generate the conformations of the saturated and partly unsaturated chains were as follows.

Saturated chains

These chains are of the form $P—(CH_2)_{n-1}—CH_3$. We have treated the headgroup as the "zeroth" carbon atom. All C—C (as well as the $P—C_1$ bond lengths were taken to be $R_{C—C} = 1.53$ Å. For ∠CCC, the angle between two successive bonds, we have used the common value $\theta = 112°$. The possible values of the rotational angles are $\varphi_k = 0, +120°$ or $-120°$ ($k = 2, 3, \cdots, n-1$), corresponding to the *trans* (t), *gauche*-plus (g^+) and *gauche*-minus (g^-) states of the kth bond. Setting the *trans* state energy $\epsilon_t \equiv 0$, the *gauche* energy is $\epsilon_g = 500$ cal/mol (for both g^+ and g^-). In generating the possible bond sequences we have discarded all the high-energy conformations, namely those involving neighboring bonds in g^+g^- or g^-g^+ states, as well as all conformations in which the nonbonded carbon atoms along the chain are less than ~3 Å apart.

Unsaturated chains

The oleoyl chains considered in the calculations $P—(CH_2)_7—CH=CH—(CH_2)_7—CH_3$, contain one *cis* double bond, between carbons C_8 and C_9. For all C—C bonds (as well as the $P—C_1$ bond) we have used $R_{C—C} = 1.53$ Å. The length of the double bond is $R_{C=C} = 1.34$ Å. For all $C_{k-1}—C_k$ bonds where $2 \le k \le 7$ and $11 \le k \le 6$ the allowed rotational angles, φ_k, are the same as for the saturated chains. The ∠CCC bond angles and *trans*/*gauche* energies of these bonds are also the same as those of the saturated chains. The differences appear in the chain segment involving carbons $C_7—C_8=C_9—C_{10}$. The angle between bonds $C_7—C_8$ and $C_8=C_9$ as well as that between $C_8=C_9$ and $C_9—C_{10}$ is $\theta = 125°$. (Note that C_7 through C_{10} are in the same plane). The possible values of the rotational angles around bonds $C_7—C_8$ and $C_9—C_{10}$ are $\varphi_8 = 0, \pm 60$ and $\varphi_{10} = 0, \pm 60$. Note that when $\varphi_8 = 0$ carbons C_6 through C_9 are in the same plane. However, the $\varphi_8 = 0$, $\varphi_{10} = 0$ configuration involves a high conformational energy and has been discarded. Thus, we have only allowed for the combinations φ_8, $\varphi_{10} = 0, \pm 60°$ or $\pm 60°, 0$ in which case $\epsilon = 800$ cal/mol or for φ_8, $\varphi_{10} = \pm 60, \pm 60$ in which case $\epsilon = 0$.

We thank professors Erich Sackmann and Klaus Schulten for helpful discussions and for explanations of their work.

The National Science Foundation administered by the Israel Academy of Science and Humanities and the Yeshaya Horowitz Association are acknowledged for financial support. The Fritz Haber Research Center is supported by the Minerva Gesellschaft für die Forschung, mbH, Munich, Germany.

REFERENCES

Andelman, D. 1994. Electrostatic properties of membranes. *In* Membranes: Their Structure and Conformations. R. Lipowsky and E. Sackmann, editors. Elsevier, Amsterdam.

Ben-Shaul, A. 1994. Molecular theory of lipid-chain packing, elasticity and lipid-protein interaction in lipid bilayers. *In* Membranes: Their Structure and Conformations. R. Lipowsky and E. Sackmann, editors. Elsevier, Amsterdam.

Ben-Shaul, A., and W. M. Gelbart. 1994. Statistical thermodynamics of amphiphile self-assembly: structure and phase transitions in micellar solutions. *In* Micelles, Monolayers, Microemulsions and Membranes. W. M. Gelbart, A. Ben-Shaul, and D. Roux, editors. Springer, New York. 1–104.

Ben-Shaul, A., I. Szleifer, and W. M. Gelbart. 1985. Chain organization and thermodynamics in micelles and bilayers. *J. Chem. Phys.* 83: 3597–3611.

Bloom, M., E. Evans, and O. G. Mouritsen. 1991. Physical properties of the fluid lipid-bilayer component of cell membranes: a perspective. *Quart. Rev. Biophys.* 24:293–397.

Büldt, G., H. U. Gally, A. Seelig, and J. Seelig. 1978. Neutron diffraction studies on selectively deuterated phospholipid bilayers. *Nature.* 271:182–184.

De Loof, H., S. C. Harvey, J. P. Segrest, and R. W. Pastor. 1991. Mean field stochastic boundary molecular dynamics simulation of a phospholipid in a membrane. *Biochem. J.* 30:2099–2113.

Dill, K. A., J. Naghizadeh, and J. A. Marqusee. 1988. Chain molecules at high densities at interfaces. *Ann. Rev. Phys. Chem.* 39:425–462.

Dill, K. A., and D. Stigter. 1988. Lateral interactions among phosphatidylcholine and phosphatidylethanolamine head groups in phospholipid monolayers and bilayers. *Biochem. J.* 27:3446–3453.

Elder, M., P. Hitchcock, R. Mason, and G. G. Shipley. 1977. A refinement analysis of the crystallography of the phospholipid, 1,2-dilauroyl-DL-phosphatidylethanolamine, and some remarks on lipid-lipid and lipid-protein interactions. *Proc. R. Soc. Lond.* 354:157–170.

Ennis, J. 1992. Spontaneous curvature of surfactant films. *J. Chem. Phys.* 97:663–678.

Fattal, D. R., and A. Ben-Shaul. 1993. A molecular model for lipid-protein interaction in membranes: the role of hydrophobic mismatch. *Biophys. J.* 65:1795–1809.

Flory, P. J. 1969. Statistical Mechanics of Chain Molecules. Wiley-Interscience, New York.

Gruen, D. W. R. 1985a. A model for the chains in amphiphilic aggregates. 1. Comparison with a molecular dynamics simulation of a bilayer. *J. Phys. Chem.* 89:146–153.

Gruen, D. W. R. 1985b. A model for the chains in amphiphilic aggregates. 2. Thermodynamic and experimental comparisons for aggregates of different shape and size. *J. Phys. Chem.* 89:153–163.

Gruen, D. W. R., and E. H. B. de Lacey. 1984. The packing of amphiphile chains in micelles and bilayers. *In* Surfactants in Solution, Vol. 1. K. L. Mittal and B. Lindman, editors. Plenum Publishing Corp., New York. 279–306.

Hauser, H., I. Pascher, R. H. Pearson, and S. Sundell. 1981. Preferred conformation and molecular packing of phosphatidylethanolamine and phosphatidylcholine. *Biochim. Biophys. Acta.* 650:21–51.

Heller, H., M. Schaefer, and K. Schulten. 1993. Molecular dynamics simulation of a bilayer of 200 lipids in the gel and in the liquid crystal phases. *J. Phys. Chem.* 97:8343–8360.

Hübner, W., H. H. Mantsch, F. Paltauf, and H. Hauser. 1994. Conformation of phosphatidylserine in bilayers as studied by fourier transform infrared spectroscopy. *Biochem. J.* 33:320–326.

Israelachvili, J. N. 1985. Intermolecular and Surface Forces. Academic Press, London.

König, S., W. Pfeiffer, T. Bayerl, D. Richter, and E. Sackmann. 1992. Molecular dynamics of lipid bilayers studied by incoherent quasi-elastic neutron scattering. *J. Phys. II France.* 2:1589–1615.

Lewis, B. A., and D. M. Engelman. 1983. Lipid bilayer thickness varies linearly with acyl chain length in fluid phosphatidylcholine vesicles. *J. Mol. Biol.* 166:211–217.

Lipowsky, R., and E. Sackmann, editors. 1994. Membranes: Their Structure and Conformations. Elsevier, Amsterdam.

Marčelja, S. 1974. Chain ordering in liquid crystals. II. Structure of bilayer membranes. *Biochim. Biophys. Acta.* 367:165–176.

Nagle, J. F., and M. C. Wiener. 1988. Structure of fully hydrated bilayer dispersions. *Biochim. Biophys. Acta.* 942:1–10.

Nagle, J. F., and D. A. Wilkinson. 1978. Lecithin bilayers, density measurements and molecular interactions. *Biophys. J.* 23:159–175.

Seelig, A., and J. Seelig. 1977. Effect of a single *cis* double bond on the structure of a phospholipid bilayer. *Biochem. J.* 16:45–50.

Seelig, J., and A. Seelig. 1980. Lipid conformation in model membranes and biological membranes. *Quart. Rev. Biophys.* 13:19–61.

Seelig, J., and N. Waespe-Šarčević. 1978. Molecular order in *cis* and *trans* unsaturated phospholipid bilayers. *Biochem. J.* 17:3310–3315.

Small, D. M. 1986. The Physical Chemistry of Lipids. Plenum Publishing Corp., New York.

Smith, S. O., I. Kustanovich, S. Bhamidipati, A. Salmon, and J. A. Hamilton. 1992. Interfacial conformation of dipalmitoylglycerol and dipalmitoylphosphatidylcholine in phospholipid bilayers. *Biochem. J.* 31:11660–11664.

Stigter, D., and K. A. Dill. 1988. Lateral interactions among phospholipid head groups at the heptane/water interface. *Langmuir.* 4:200–209.

Szleifer, I., A. Ben-Shaul, and W. M Gelbart. 1985. Chain organization and thermodynamics in micelles and bilayers. II. Model calculations. *J. Chem. Phys.* 83:3612–3620.

Szleifer, I., A. Ben-Shaul, and W. M. Gelbart. 1987. Statistical thermodynamics of molecular organization in mixed micelles and bilayers. *J. Chem. Phys.* 86:7094–7109.

Szleifer, I., D. Kramer, A. Ben-Shaul, W. M. Gelbart, and S. A. Safran. 1990. Molecular theory of curvature elasticity in surfactant films. *J. Chem. Phys.* 92:6800–6817.

Tanford, C. 1980. The Hydrophobic Effect, 2nd ed. Wiley-Interscience, New York.

van der Ploeg, P., and H. J. C. Berendsen. 1983. Molecular dynamics of a bilayer membrane. *Mol. Phys.* 1:233–248.

Wennerström, H., and B. Lindman. 1979. Micelles, physical chemistry of surfactant association. *Phys. Rep.* 52:1–86.

Wiener, M., C., and S. H. White. 1992a. Structure of a fluid dioleoylphosphatidylcholine bilayer determined by joint refinement of x-ray and neutron diffraction data. II. Distribution and packing of terminal methyl groups. *Biophys. J.* 61:428–433.

Wiener, M., C., and S. H. White. 1992b. Structure of a fluid dioleoylphosphatidylcholine bilayer determined by joint refinement of x-ray and neutron diffraction data. III. Complete structure. *Biophys. J.* 61:434–447.

Wilkinson, D. A., and J. F. Nagle. 1981. Dilatometry and calorimetry of saturated phosphatidylethanolamine dispersions. *Biochem. J.* 20: 187–192.

Winterhalter, M., and W. Helfrich. 1992. Bending elasticity of electrically charged bilayers: coupled monolayers, neutral surfaces, and balancing stresses. *J. Phys. Chem.* 96:327–330.